Proceedings of the ASME 2025
International Design Engineering Technical Conferences and Computers and Information in Engineering Conference
IDETC/CIE2025
August 17–20, 2025, Anaheim, CA

IDETC2025-168930

END-OF-LIFE PREDICTION FOR SOLDER JOINTS IN ELECTRONIC SYSTEMS EXPERIENCING LOW-CYCLE FATIGUE UNDER IMPACT LOADING

Zhymir Thompson[1,2], Ryan Yount[1], Jacob Dodson[3], Adriane Moura[4], Austin R.J. Downey[1,5,*]

[1]Department of Mechanical Engineering, University of South Carolina, Columbia, SC
[2]Department of Computer Science and Engineering, University of South Carolina, Columbia, SC
[3]Air Force Research Laboratory, Munitions Directorate, Eglin Air Force Base, FL
[4]Applied Research Associates, Emerald Coast Division, Niceville, FL
[5]Department of Civil and Enviromental Engineering, University of South Carolina, Columbia, SC

1. ABSTRACT

Electronic assemblies, especially composite printed circuit boards, frequently operate in environments characterized by high-rate dynamic loads, such as impacts and shocks, posing significant challenges for predicting their end-of-life. Traditional life prediction methodologies typically estimate time-to-failure, which may not be sufficient for systems experiencing intermittent but intense loading events. This paper introduces an improved predictive maintenance approach for estimating the remaining useful life of solder joints in electronic assemblies subjected to low-cycle fatigue under repeated high-energy impact loading. The proposed methodology employs strain-life fatigue analysis combined with rain-flow counting and equivalent cycle counting techniques, specifically tailored for assessing cumulative damage in solder joints of printed circuit boards. This is accomplished through the use of solder properties calculated for the assumed operating environment and by using a unitless proportional damage to describe damage accrued from a particular impact event. The developed algorithm uses acceleration data from impact tests to estimate strain through empirical relationships, enabling a robust evaluation of fatigue accumulation in solder joints. Experimental validation was conducted using cantilevered composite printed circuit boards subjected to repeated, high-energy drop tests designed to induce low-cycle fatigue. Results indicate that the proposed method successfully predicts cumulative damage and accurately estimates solder joint failure due to fatigue.

2. INTRODUCTION

Blasts against civil structures, automotive crashes, and high-speed aircraft are all examples where structures are subjected to sudden large forces. These events can be characterized as high-rate dynamics. Structures experiencing high-rate dynamics are those that experience high acceleration or de-acceleration of greater than 100 g_n on a time scale of less than 1 ms [1]. In an ideal case, a high-rate dynamic event may manifest itself as a single shock event. Structures are limited in how many repeated shock events they can endure. Structures under shock loading can fail suddenly [2]. This can lead to hazardous situations and require expensive repairs which cost time and money. Forecasting the remaining useful life (RUL) for a structure would enable the implementation of control schemes or repairs that would reduce the likelihood of a sudden failure occurring while the structure is in service. In this way, forecasting RUL for a structure improves safety and reduces maintenance costs.

Electronics components and assemblies can likewise be subjected to high-rate dynamic environments. Estimating the RUL for these components can help in maximizing their performance over the lifetime of a system. Solder joint failure is a substantial point of failure for electronic components [3, 4]. Furthermore, the low strength of solder bonds means components are more likely to detach when subjected to high shock loadings. Not only are detached components useless for functionality in electronics, but they also have the potential to damage other components or cause short circuits where they migrate. For these reasons, it is desirable to estimate reliably the remaining damage that a component could endure before failing. In addition, an ideal implementation of the estimate would be usable in situations where damaging events may be separated by a time-invariant variable.

Similar to the durability mechanic in some video games, fatigue analysis can be used to estimate the remaining life of a structure or electronic system. As an example, Palmgren-Miner's rule can be used to give "a linearized estimate of the damage induced by a single fatigue cycle" [5]. An estimate of the accumulated damage can be tracked over the lifetime of a structure.

*Corresponding author

A great amount of effort has gone into predicting the damage caused by fatigue. That effort has extended into fatigue in electronics to investigate damage from conditions like thermal cycling [5]. Many models and equations have been created to predict damage to electronics and solder in particular. Among other things, they have characterized the properties of solder, factors that affect solder lifetime, and the initiation and propagation of cracks in solder. There have also been attempts to model damage to solder with mathematical equations. Basaran et al. [6] investigated the growth of grains in a lead-based solder used in ball-grid arrays. Grain growth is an important factor in determining the lifespan of solder. As grains get larger, the solder becomes more susceptible to failure. They found that temperature and strain were the factors that affected the rate of grain growth in lead-based solder. Libot et al. [7] performed tests on lead-free solder to analyze failure points and damage in solder joints. These joints were subjected to mechanical stress at different temperatures with different loading conditions. In part, they observed that failure in solder would occur in the bulk material and grow along the junction where the solder was connected to another material. Kim et al. [8] also looked at damage to lead-free solder joints. These lead-free solder joints were part of a ball-grid array configuration. They also found that damage occurred primarily towards the junction connecting the solder to other components. These observations and corresponding equations show that grain growth is an important factor in determining the remaining life of solder. Temperature and strain were found to be contributing factors to solder damage. The inevitable failure of the solder is fairly consistent in that it is primarily due to cracks that propagate along the connection between the solder and the attached component. Along with contributions that analyze solder, other works have used the ideas of fatigue theory to model damage.

Similar approaches have been taken for estimating remaining life in batteries [9, 10]. Zhao et al predicted the remaining useful life (RUL) of lithium-ion batteries using a combination of deep belief network and relevance vector machine. The battery data was passed into the deep belief network to extract useful features. The features were fed into the relevance vector machine to predict remaining life while incorporating uncertainty into the model [9]. Motapon et al constructed a physics-based cycle life model for lithium-ion batteries using fatigue theory and equivalent cycle counting [10]. A cycle life model was used to calculate battery degradation from cycles of charge and discharge. The charging and discharging of the battery were treated as fatigue damage to the battery. The proportional damage from cycles where the battery was not fully charged or discharged was calculated using equivalent cycle counting. This approach simplified modeling battery degradation, and the model could be generalized to different lithium-ion batteries since the simplified model used physics-based equations applicable to all lithium-ion batteries.

Fatigue can be modeled in a number of ways. The strain-life method is the method of interest in this work. The strain-life method is useful for detecting the amount of damage that a structure can sustain before a crack develops. This method is particularly useful for low-cycle fatigue where plastic deformation is expected to occur [11]. Wong et al performed a review of creep-fatigue models for solder joints [5]. They discuss the theory of creep and fatigue, a number of fatigue models, and the performance metrics for the different models.

In this work, fatigue analysis is used for estimating the life of solder joints using properties of solder measured in previous experiments. By using equivalent cycle counting, the damage estimate produced may be converted to a variety of suitable forms including the natural frequency of the material. This is accomplished by converting the unitless output of damage calculation to a number of cycles of strain. Data for this work is available through a public repository [12]. The contribution of this work is the formulation of an algorithm to estimate the remaining life for solder between a PCB and electronic component. The algorithm uses fatigue analysis and equivalent cycle counting to convert sequential data to an estimate of damage for a system of interest.

3. BACKGROUND

Fatigue is defined as "the process of cumulative damage. . . caused by repeated fluctuating loads. . . " [13]. Fatigue is damage over time. Structures subjected to periodic loading and unloading accrue damage. As the cycles of loading continue, the structure becomes increasingly more damaged until reaching a point of failure. When a structure is near this point, it can break suddenly even under loads less than its initial load rating.

The elastic strain range is defined by Equation 1. $\Delta\varepsilon_e$ is elastic strain range, K is strength coefficient, E is modulus of elasticity, N is number of material reversals, and B_0 is strength exponent. Elastic strain is linearly proportional to the applied load, and it decreases to a baseline threshold once the load is removed.

$$\frac{\Delta\varepsilon_e}{2} = \frac{K}{E} \cdot (2N)^{-B_0} \tag{1}$$

The plastic strain range is defined by Equation 2. $\Delta\varepsilon_p$ is plastic strain range, ϵ_f is ductility coefficient, β_0 is ductility exponent.

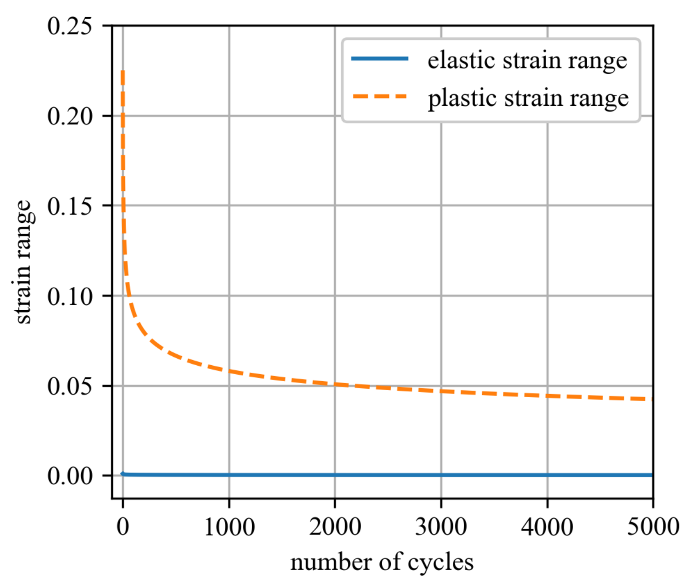

FIGURE 3: EXAMPLE STRAIN-LIFE CURVE. THE CURVE SHOWS SEPARATELY THE ELASTIC AND PLASTIC CONTRIBUTIONS TO TOTAL FATIGUE FOR A STRUCTURE.

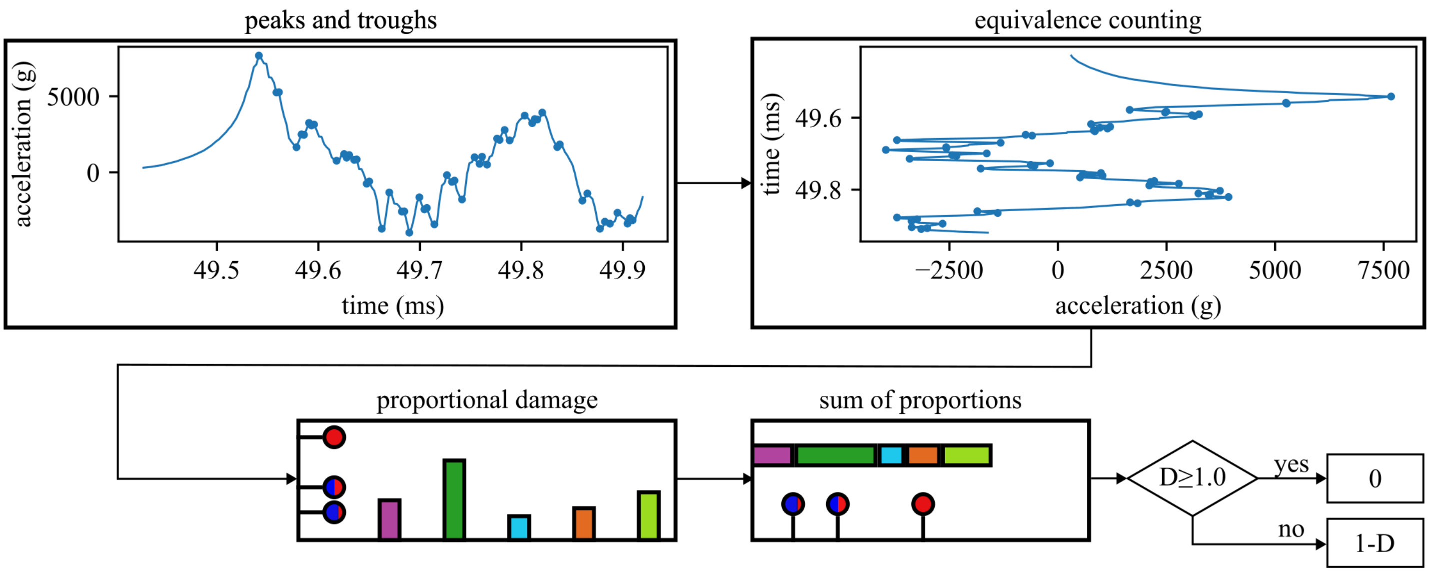

FIGURE 1: FLOWCHART SHOWING THE PROCESS FOR CALCULATING THE DAMAGE FOR THE STRUCTURE.

TABLE 1: TABLE OF SOLDER PROPERTIES COLLECTED FOR EXPERIMENTS.

Solder (ISO)	Modulus of elasticity	Strength coefficient	Strength exponent	Ductility coefficient	Ductility exponent
(SAC711)	5.1×10^{10} Pa	4.9×10^{7}	1.608×10^{-1}	2.25×10^{-1}	1.96×10^{-1}

It is nonlinear in nature and results in a permanent alteration to the structure.

$$\frac{\Delta\varepsilon_p}{2} = \epsilon_f \cdot (2N)^{-\beta_0} \tag{2}$$

Equation 3 shows that the total strain range is the sum of the elastic and plastic strain ranges. The elastic strain contributes more and thus dominates the relationship when the strain is lower. The plastic strain dominates when the strain is higher. Elastic strain contributes more to the damage in high-cycle fatigue and plastic strain contributes more to damage in low-cycle fatigue.

$$\frac{\Delta\epsilon}{2} = \frac{\Delta\varepsilon_e}{2} + \frac{\Delta\varepsilon_p}{2} \tag{3}$$

Substituting Equation 1and Equation 2 into Equation 3 gives Equation 4.

$$\frac{\Delta\epsilon}{2} = \frac{K}{E} \cdot (2N)^{-B_0} + \epsilon_f \cdot (2N)^{-\beta_0} \tag{4}$$

Equation 4 is the relation used in this work to predict cycles to failure for a given structure. This work is primarily focused on damage induced during low-cycle fatigue, so it would be reasonable to assume that the damage from elastic strain would be negligible. While it is true that plastic strain dominates low-cycle fatigue, the elastic strain should not be completely disregarded.

Figure 3 shows an example of a strain-life curve. For the range of interest, the plastic strain dominates the relation, as expected for low-cycle fatigue. In a dynamic setting, a structure may undergo long periods of low amplitude stress with sparse high amplitude impacts. The structure still experiences wear that affects performance in the low amplitude settings, so ignoring the contribution of elastic strain would remove important information depending on the timescale of data. Along with comparing the contributions of elastic and plastic strain to fatigue, the curves depicted in Figure 3 are used in estimating damage to a structure.

The strain-life method uses strain range to predict the number of cycles to failure. For this method, failure is defined as the development of a crack. This method uses a strain-life curve to map strain ranges to their respective number of cycles to failure. The strain-life curve represents the number of cycles of load that a structure could withstand if each cycle of load-induced the respective amount of strain. The strain-life curve is a powerful tool for estimating life expectancy, but one disadvantage is that the curve assumes that the strain of the material is consistent. The Miner's rule is commonly used to extend this damage calculation to dynamic loading conditions.

4. METHODOLOGY

Figure 1 is a flowchart detailing the steps of the algorithm. A sequence of data is taken as input. The peaks and troughs for the data are extracted as a sequence from the data. The rain flow counting method is used to convert the peaks and troughs to equivalence cycles. The cycles represent fatigue at various cyclic loads. Essentially, the cycles of the original signal are separated and rearranged so that cycles with the same range are counted together. The total number of cycles to failure for any given strain range can be found with a stress-strain curve. By

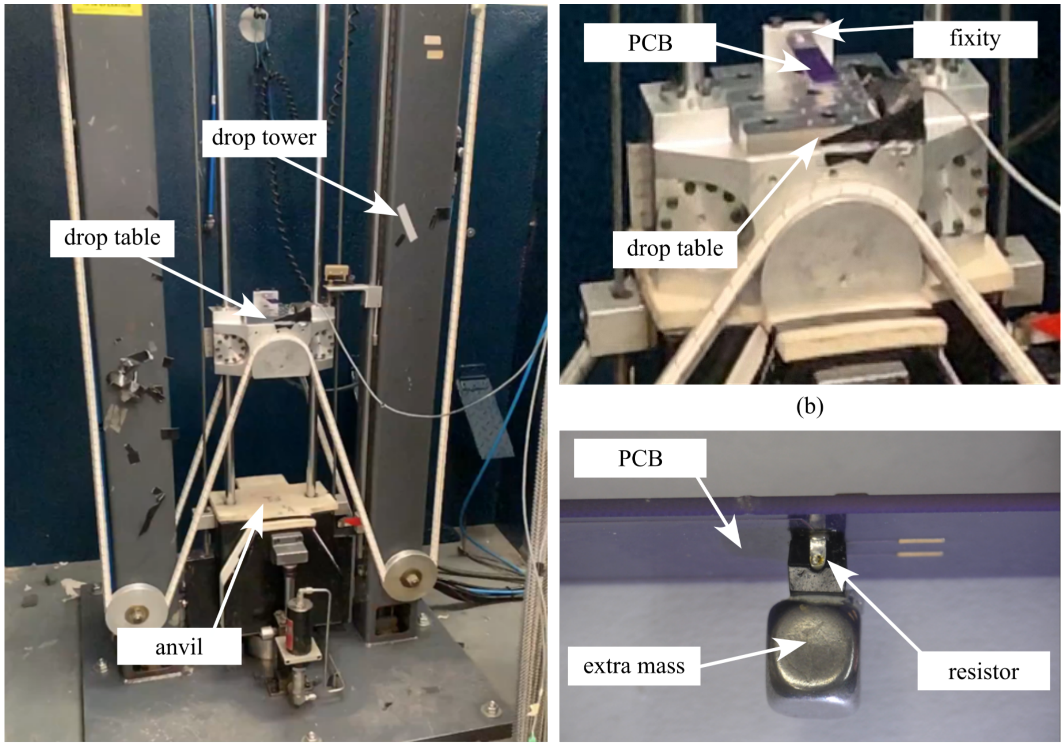

(a) (b) (c)

FIGURE 2: EXPERIMENTAL SETUP USED FOR THE EXPERIMENT, SHOWING (A) THE DROP TOWER SYSTEM; (B) THE PCB EXPERIMENTAL SETUP ON THE DROP TABLE, AND; (C) THE RESISTOR ATTACHED TO THE PCB WITH A WEIGHT ATTACHED TO THE RESISTOR.

converting counts of cycles at each strain range into fractions, the fraction of total damage for each strain range can be calculated. This is calculated by taking the proportion of the number of cycles given by equivalence counting compared to their respective number of cycles for total damage. Then, these proportions of damage can be added together. If this sum of proportional damage reaches or exceeds 1, then the accrued damage suggests that the structure has failed. Otherwise, the structure still remains viable, and the remaining durability of the structure is equivalent to the remaining percentage of damage that the structure can endure. This algorithm uses Palmgren Miner's rule and inherits its assumptions and limitations. The rule assumes that the order of cycles does not affect the damage accrued. This is not always true in practice. For example, a high-force impact followed by low-force impacts could lead to a lower RUL than in the reverse-case if the high-force impact results in plastic deformation.

The experimental setup utilized the shock test system depicted in Figure 2. The PCB and associated components were securely mounted to the table within the test apparatus. To generate the desired impact, the system was elevated to a specific height and released, allowing it to free fall and strike the surface below. During each impact, acceleration and strain data were continuously recorded from a piezoresistive accelerometer and two strain gauges respectively to capture the system's response to the induced shock. As an electrical reference and failure time reference, a resistive circuit was employed. The resistive circuit was comprised of a voltage divider circuit and a data acquisition line to record voltage drop across the resistor.

Part (c) of Figure 2 provides a close-up view of the component of interest on the 2.5-inch rectangular cantilever PCB. The component under investigation is the resistor used in the resistive circuit, mounted to the PCB using SAC711 lead-free solder, with a small weight attached to promote failure at the solder joint. The purpose of the experiment was to detect the failure of this solder connection between the resistor and the PCB. To ensure that the solder joint would fail before any other component, the attached weight was used to induce extra stress at the desired location. The procedure involved repeated shock tests, incrementally increasing the applied shock in units of gravities until the solder joint failed and the resistor detached. Each shock event represents a discrete impact over time, contributing to cumulative damage to the solder joint. This process is alike bending a paper clip back and forth as although time passes between bends, the accumulated damage remains and ultimately leads to failure.

Five solder properties were needed to estimate damage using the strain-life method: modulus of elasticity, strength coefficient, strength exponent, ductility coefficient, and ductility exponent. Some of these properties could be collected from existing tables of material properties. Some other properties could be inferred through relationships between the variables. The remaining properties are typically collected empirically, so they were obtained from findings in other works [8]. The solder used for this experiment was common enough to have been studied well in literature and common material parameters are reported in Table 1. The solder properties used in this algorithm are dependent on a number of factors. Factors that affect solder properties include tem-

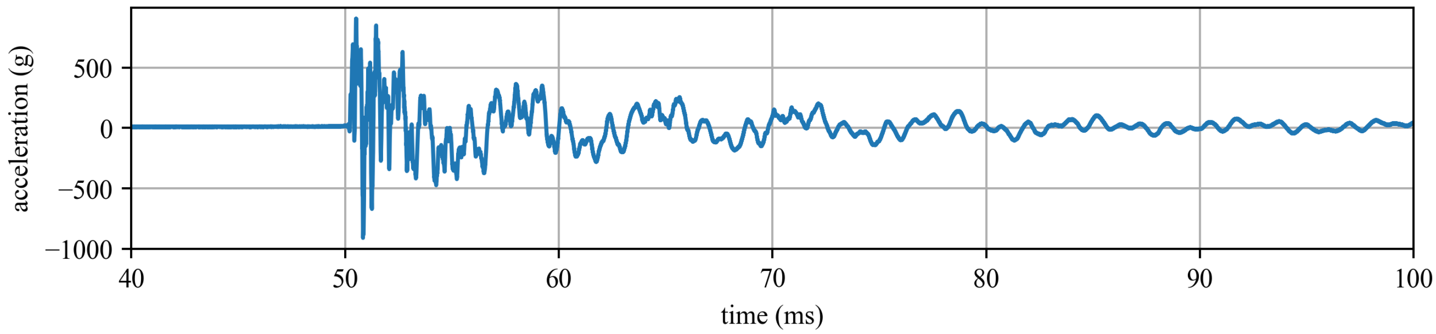

FIGURE 4: ACCELERATION DATA COLLECTED FROM A TEST IMPACT OF THE BOARD.

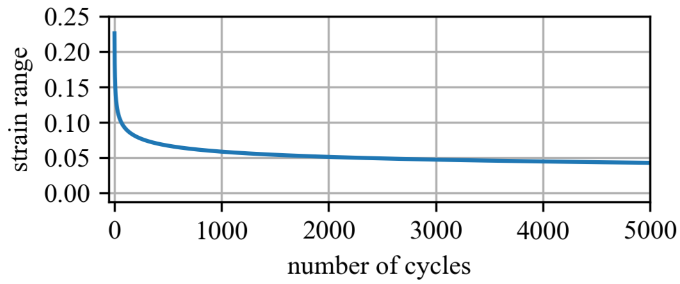

FIGURE 5: STRAIN-LIFE CURVE FOR SOLDER SAC711; USING VARIABLES FROM TABLE 1.

perature, cyclic loading frequency, shape, size, etc. This means that finding these properties for a particular material can be somewhat involved, either requiring considerable testing or an in-depth search of reference material. There are other fatigue equations that take into account some of these factors (i.e. temperature and cyclic loading) [5], but generally these properties must be found for a particular environment and context.

An example of the acceleration data collected in an experiment run is shown in Figure 4. The acceleration plot shows the response of the system to a great impact exceeding 750 g_n's of force. The acceleration shown is representative of the damage that the system receives during the experiment. The large amplitude response is noteworthy in determining overall fatigue, but the bending caused by subsequent vibrations also has an effect on the overall damage. This work is interested in the effect of the large amplitude and lower amplitude vibrations of the component over multiple runs of the experiment.

The data collected though did not include strain at the point of the resistor. Strain at the point of the resistor is needed to estimate the number of cycles until failure. So to calculate the strain at the point of the resistor, Equation 5 was used to convert acceleration to strain. The equation

$$\varepsilon = \frac{F}{A \cdot E} \tag{5}$$

describes the relationship between force and strain. F is force, A is the cross-sectional area of the beam, and E is the modulus of elasticity. Converting force yields

$$\varepsilon = \frac{m \cdot a}{A \cdot E} \tag{6}$$

where ε is strain, m is the mass of the PCB and attached components, and a is acceleration. All of the values in Equation 6 are known or measured except mass. This logic assumes that the force of interest can be converted to the product of mass and acceleration. While this assumption may not be true, we can assume that force is proportional to strain.

The prediction of the algorithm was off when Equation 6 was used directly. To correct for this, a coefficient was introduced. The coefficient would scale the acceleration data to better convert acceleration data to strain data. A minimization process was used to estimate the coefficient which was then used to transform the acceleration to strain. The approximate strain was compared to the other experimental runs. The coefficient was found by using acceleration data that was known to lead to failure to estimate the scalar.

The curve depicted in Figure 5 shows the relationship between the strain range for the solder and the number of cycles until failure. The curve is the sum of two exponentials as defined by the coffin-manson relation shown in Equation 4.

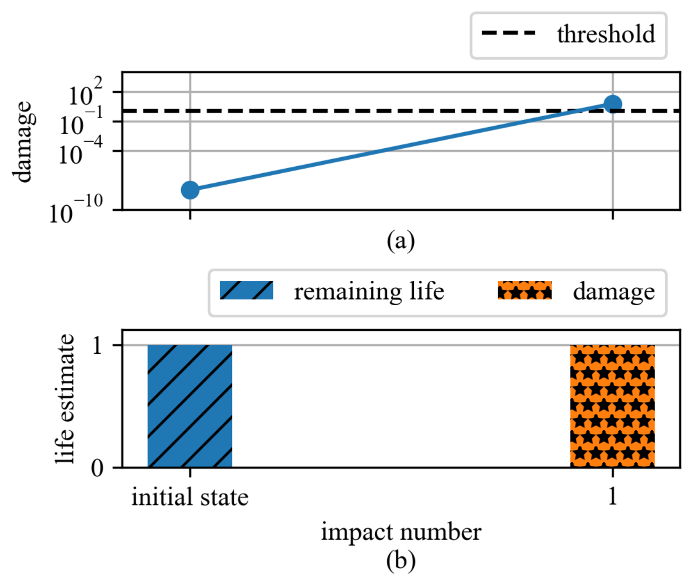

FIGURE 6: ACCUMULATED DAMAGE FOR SET 1, SHOWING: (A) TOTAL DAMAGE AT END OF EACH IMPACT AND; (B) PROPORTION OF RUL FOR STRUCTURE.

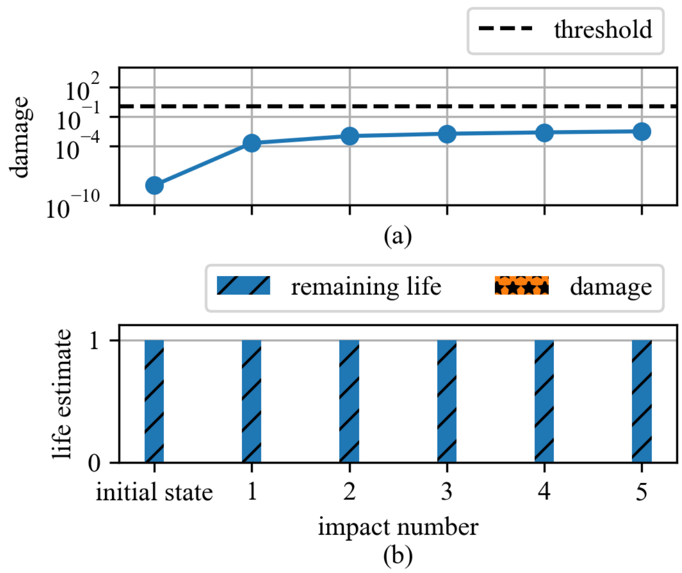

FIGURE 7: ACCUMULATED DAMAGE FOR SET 2, SHOWING: (A) TOTAL DAMAGE AT END OF EACH IMPACT AND; (B) PROPORTION OF RUL FOR STRUCTURE.

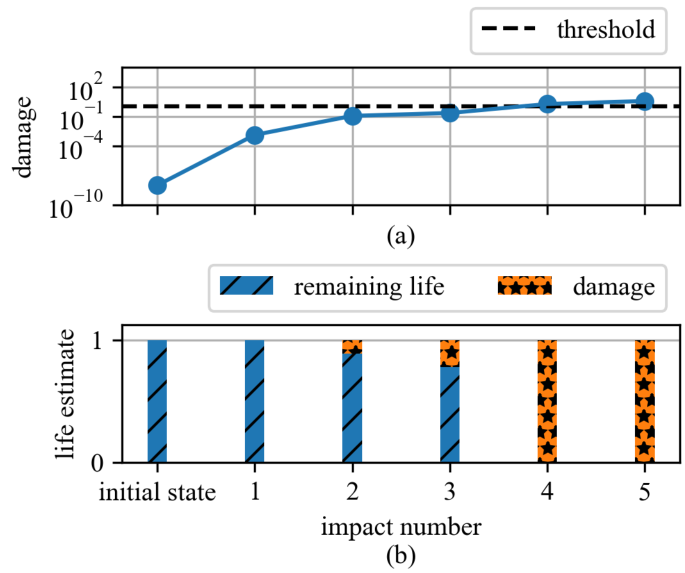

FIGURE 8: ACCUMULATED DAMAGE FOR SET 3, SHOWING: (A) TOTAL DAMAGE AT END OF EACH IMPACT AND; (B) PROPORTION OF RUL FOR STRUCTURE.

The experiments consisted of repeated impacts of a test apparatus until the resistor separated from the PCB. The goal of the experiment was to damage the PCB enough that a component attached to the PCB failed. The predicted failure was defined as the solder between the resistor and solder pads separating. In total, there were three test sets, each tested to failure.

5. RESULTS

The algorithm predicted the RUL after every impact. A graph was made for each of the test sets, these are Figures 6-8. The test specimen failed during the last reported impact in each test set. The graphs depict RUL predictions by the algorithm after each impact. A new PCB was used for every test set.

Figure 6 was test set 1. The graph in Figure 6(a) shows the accumulated damage for the first run. Moreover, Figure 6(b) reports, as a bar plot, the life estimate for the test specimen before each impact. This PCB failed after one impact, therefore a second impact was not undertaken. As this test set ended after one impact, it serves as evidence that the algorithm works in the base case and that the coefficient estimated prior was a good approximation. This test set was the only one that ended after one impact. Later test sets involved impacts with less force, so the PCBs survived longer without requiring replacement.

Test set 2 is shown in Figure 7. As shown in Figure 7(a), the algorithm developed in this work calculated that minimal damage had occurred. Figure 7(b) shows the algorithm predicted that the test device suffered minimal damage over the series of impacts. In fact, the algorithm predicted that the component had near 100% RUL. Despite what is predicted by the algorithm, the resistor fell off earlier than estimated. The failure for this run was due to a failure at the solder-pad/PCB interface rather than the modeled solder failure. As the proposed algorithm only provides RUL predictions for failure in the solder connection between the resistor and solder pad, it does not make predictions for failure due to defects and damage to the connection between the solder pad and PCB. Therefore, the discrepancy reported in Figure 7 does not provide concrete information about the proposed algorithm.

Figure 8 reports results for test set 3. As seen in Figure 8(a) and (b) the algorithm predicted damage would build up after impact 2 and that failure would occur at the end of the 4th impact. In reality, the resistor managed to survive until the 5th impact. The specific cause of the early predicted failure is unknown. Regardless, the component survived only a single impact more than expected, so the algorithm made a fairly accurate prediction.

6. CONCLUSION

In this work, we designed an algorithm to transform sequential acceleration into an estimation of life for solder joints subjected to impacts. The algorithm can estimate the remaining life for electronics where components are expected to break suddenly after a relatively small number of impacts. By estimating how much longer an electronic component can be expected to perform, one can make decisions about future actions prior to component failure. Thus, appropriate prediction allows for action to future failure as opposed to reaction to imminent failure. The impacts were separated into individual files for this experiment. An algorithm that could separate continuously measured data into meaningful impacts could use the estimated damage to predict remaining survivable impacts of similar force.

The algorithm presented good performance and revealed potential limitations. The algorithm only makes predictions for a single component. This may be desired if interest is primarily in the lifespan of a single component. One could construct multiple models to run concurrently as a potential solution. Another limitation is that the current model uses variables that vary with temperature. Replacing the model in the algorithm with one that could account for the variation would likely improve performance and flexibility for varying environmental conditions. Future work will involve incorporating fatigue due to creep into the algorithm. It is expected that accounting for creep when determining fatigue will provide a more accurate model. The model would also allow for determining fatigue under variable conditions.

Verification of the proposed method is certainly an important consideration. The model makes assumptions that could be incorrect depending on the context. The model could also simply be uninformative in a different environment. There are two possible methods to validate model correctness. The first option would be to use Finite Element Analysis (FEA) to simulate an object subjected to impact. The second option would be to measure strain across the surface of an object. Both cases can be used to compare the calculated or measured strain to the estimate computed by the proposed algorithm. FEA would almost certainly give better results for the particular location of interest, but strain measurement would give results more aligned with real-world measurements.

To verify that the model is informative, one could compare the life estimate to crack length along the solder/solder pad junction. The crack length should not increase by more than a negligible amount until the RUL reaches zero. Finding the crack length is somewhat difficult in practice. The easiest path would likely be to use FEA to calculate the crack length for a simulation. Alternatively, one could also scan the surface where the PCB is attached to detect surface reading changes that could indicate a crack. Finally, one could use a high-speed camera or similar setup to visually check for a gap formation indicating a crack.

7. ACKNOWLEDGMENTS

This material is based upon work supported by the Air Force Research Lab through the summer scholars program. Additional support from the Air Force Office of Scientific Research (AFOSR) through award no. FA9550-21-1-0083 and the National Science Foundation grant numbers CCF - 1937535, CCF - 1956071, CCF-2234921, and CPS - 2237696, Any opinions, findings conclusions, or recommendations expressed in this material are those of the authors and do not necessarily reflect the views of the United States Air Force or the National Science Foundation DISTRIBUTION STATEMENT A. Approved for public release: distribution unlimited. (AFRL-2024-5027).

REFERENCES

[1] Dodson, Jacob, Downey, Austin, Laflamme, Simon, Todd, Michael D., Moura, Adriane G., Wang, Yang, Mao, Zhu, Avitabile, Peter and Blasch, Erik. *High-Rate Structural Health Monitoring and Prognostics: An Overview*. Springer International Publishing (2021): pp. 213–217. DOI 10.1007/978-3-030-76004-5_23.

[2] Lall, P., Choudhary, P., Gupte, S. and Suhling, J. "Health Monitoring for Damage Initiation and Progression during Mechanical Shock in Electronic Assemblies." *56th Electronic Components and Technology Conference 2006*: pp. 85–94. IEEE. DOI 10.1109/ectc.2006.1645630.

[3] Pang, John H.L., Xiong, B.S. and Low, T.H. "Low cycle fatigue models for lead-free solders." *Thin Solid Films* Vol. 462–463 (2004): pp. 408–412. DOI 10.1016/j.tsf.2004.05.037.

[4] Sharon, Gilad. "Temperature Cycling and Fatigue in Electronics." .

[5] Wong, E.H., van Driel, W.D., Dasgupta, A. and Pecht, M. "Creep fatigue models of solder joints: A critical review." *Microelectronics Reliability* Vol. 59 (2016): pp. 1–12. DOI 10.1016/j.microrel.2016.01.013.

[6] Basaran, C. and Wen, Yujun. "Grain growth in eutectic Pb/Sn ball grid array solder joints." *ITherm 2002. Eighth Intersociety Conference on Thermal and Thermomechanical Phenomena in Electronic Systems (Cat. No.02CH37258)*, Vol. eep: pp. 903–908. IEEE. DOI 10.1109/itherm.2002.1012551.

[7] Libot, J. B., Arnaud, L., Dalverny, O., Alexis, J., Milesi, P. and Dulondel, F. "Mechanical fatigue assessment of SAC305 solder joints under harmonic and random vibrations." *2016 17th International Conference on Thermal, Mechanical and Multi-Physics Simulation and Experiments in Microelectronics and Microsystems (EuroSimE)*: pp. 1–8. 2016. IEEE. DOI 10.1109/eurosime.2016.7463294.

[8] Kim, Choong-Un, Bang, Woong-Ho, Xu, Huili and Lee, Tae-Kyu. "Characterization of Solder Joint Reliability Using Cyclic Mechanical Fatigue Testing." *JOM* Vol. 65 No. 10 (2013): pp. 1362–1373. DOI 10.1007/s11837-013-0720-2.

[9] Zhao, Guangquan, Zhang, Guohui, Liu, Yuefeng, Zhang, Bin and Hu, Cong. "Lithium-ion battery remaining useful life prediction with Deep Belief Network and Relevance Vector Machine." *2017 IEEE International Conference on Prognostics and Health Management (ICPHM)*: pp. 7–13. 2017. IEEE. DOI 10.1109/icphm.2017.7998298.

[10] Motapon, Souleman N., Lachance, Enric, Dessaint, Louis-A. and Al-Haddad, Kamal. "A Generic Cycle Life Model for Lithium-Ion Batteries Based on Fatigue Theory and Equivalent Cycle Counting." *IEEE Open Journal of the Industrial Electronics Society* Vol. 1 (2020): pp. 207–217. DOI 10.1109/ojies.2020.3015396.

[11] Harris, Cyril M. and Piersol, Allan G. (eds.). *Harris' shock and vibration handbook*, 5th ed. McGraw-Hill handbooks, McGraw-Hill, New York [u.a.] (2002). Previous ed.: 1996.

[12] Yount, Ryan, Dodson, Jacob and Moura, Adriane. "Dataset 9 Repeated Impact Testing of Rectangular Electronic Assembly." URL https://github.com/High-Rate-SHM-Working-Group/Dataset-9-repeated-impact-testing-of-rectangular-electronic-assembly.

[13] Barsom, John M and Rolfe, S. T. (eds.). *Fracture and fatigue control in structures*, 3rd ed. No. MNL 41-3RD in *ASTM manual series*, ASTM, West Conshohocken, PA (1999). In: Knovel library. - Dateiformat Volltext: PDF. - Includes bibliographical references and index. - Print version record.